25-Hydroxycholesterol Increases the Availability of Cholesterol in Phospholipid Membranes

Brett N. Olsen,[†] Paul H. Schlesinger,[‡] Daniel S. Ory,[§] and Nathan A. Baker[¶*]

[†]Department of Medicine, Diabetic Cardiovascular Disease Center, Washington University School of Medicine, St. Louis, Missouri; [‡]Department of Cell Biology and Physiology, Washington University in St. Louis, St. Louis, Missouri; [§]Diabetic Cardiovascular Disease Center, Washington University School of Medicine, St. Louis, Missouri; and [¶]National Security Directorate, Pacific Northwest National Laboratory, Richland, Washington

ABSTRACT Side-chain oxysterols are enzymatically generated oxidation products of cholesterol that serve a central role in mediating cholesterol homeostasis. Recent work has shown that side-chain oxysterols, such as 25-hydroxycholesterol (25-HC), alter membrane structure in very different ways from cholesterol, suggesting a possible mechanism for how these oxysterols regulate cholesterol homeostasis. Here we extend our previous work by using molecular-dynamics simulations of 25-HC and cholesterol mixtures in 1-palmitoyl-2-oleoyl-phosphatidylcholine bilayers to examine the combined effects of 25-HC and cholesterol in the same bilayer. 25-HC causes larger changes in membrane structure when added to cholesterol-containing membranes than when added to cholesterol-free membranes. We also find that the presence of 25-HC changes the position, orientation, and solvent accessibility of cholesterol, shifting it into the water interface and thus increasing its availability to external acceptors. This is consistent with experimental results showing that oxysterols can trigger cholesterol trafficking from the plasma membrane to the endoplasmic reticulum. These effects provide a potential mechanism for 25-HC-mediated regulation of cholesterol trafficking and homeostasis through modulation of cholesterol availability.

INTRODUCTION

Biological membranes are a complex mixture primarily composed of phospholipids, sterols, and proteins. These constituents contribute to the basic physical structure and behavior of membranes. Cholesterol (Fig. 1 *A*) is the most prominent sterol in mammalian membranes, with some membranes containing up to 50% cholesterol (1,2). Cholesterol is distributed asymmetrically within cells, with the plasma membrane containing a much higher concentration than internal membranes such as the endoplasmic reticulum (ER) and the Golgi (1–3). Cholesterol is required by all mammalian cells and serves multiple functions, such as regulating protein behavior through direct binding to sterol-sensing domains (4–6) and serving as a precursor for steroid hormone and bile acid synthesis (7). In addition to its direct effects within membranes, cholesterol also alters the structure and behavior of the membranes themselves. Biophysical and simulation studies have shown that the addition of cholesterol to membranes decreases membrane fluidity while increasing membrane thickness, bending modulus, and lipid order (8–13), even without forming distinct domains, and plays an important role in the formation of lipid rafts (14,15). These indirect effects influence cellular behavior; for example, increases in membrane thickness caused by high levels of cholesterol are thought to help sort membrane proteins between the Golgi and the plasma membrane (16), and membrane structural changes can alter ion channel properties (17) and influence protein signaling (15).

Because of the importance of cholesterol for cellular function, cholesterol levels in cell membranes are kept under tight control by multiple sterol-regulated pathways. Transcriptional regulation of cholesterol homeostasis occurs through both sterol regulatory element-binding protein (SREBP)-controlled genes (18,19) and liver X receptor (LXR)-controlled genes (20,21). Although most cellular cholesterol is located in the plasma membrane, key cholesterol homeostatic functions occur primarily in the ER, where SREBP, HMG-CoA reductase, and acyl CoA acyltransferase reside (19,22–26). This suggests that cholesterol homeostasis is primarily determined by the ER cholesterol concentration rather than by the total cellular cholesterol concentration (27). In turn, the ER membrane cholesterol content is regulated by the brisk exchange of cholesterol between the plasma membrane and the ER. According to the active cholesterol hypothesis, the availability of cholesterol for transfer between membranes is determined by its partitioning between two pools: a complexed pool that is tightly bound to phospholipids, and an activated pool that is not tightly bound and hence is more accessible to other cholesterol-binding molecules for transfer to internal membranes (27,28).

Side-chain oxysterols, such as 25-hydroxycholesterol (25-HC; see Fig. 1 *B*), are known to trigger cholesterol trafficking from the plasma membrane to the ER (29). We propose that side-chain oxysterols promote the activation of cholesterol. Addition of exogenous oxysterols to the plasma membrane greatly increases the number of activated cholesterol molecules, triggering their movement to the ER. Likewise, under physiological conditions, oxysterols in the

Submitted July 13, 2010, and accepted for publication December 8, 2010.

*Correspondence: nathan.baker@pnl.gov

Editor: Scott Feller.

© 2011 by the Biophysical Society

0006-3495/11/02/0948/9 $2.00

doi: 10.1016/j.bpj.2010.12.3728

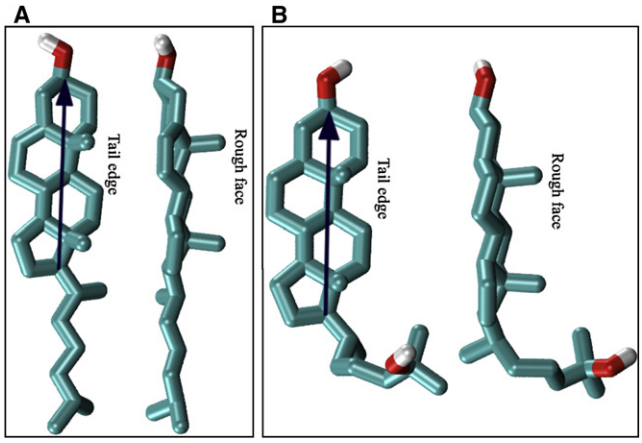

FIGURE 1 Structures of cholesterol (*A*) and 25-HC (*B*). Arrows show the direction of the sterol axis, from carbon 17 to carbon 3. Edges and faces of the steroid rings are shown. The tail edge of the sterol is defined as the edge from which the sterol tail extends, and the rough face of the sterol is defined as the face from which the two methyl groups project.

ER promote the interaction of cholesterol with sterol-sensing proteins, which partially explains their ability to signal in cholesterol homeostatic pathways (27–33). In this work, we present evidence from molecular dynamics (MD) simulations that cholesterol and oxysterols interact indirectly within membranes, with oxysterols disrupting the ability of cholesterol to condense membrane bilayers and causing changes in cholesterol positioning consistent with cholesterol activation.

MATERIALS AND METHODS

Parameters, starting structures, and simulation details

The cholesterol, 25-HC, and 1-palmitoyl-2-oleoyl-phosphatidylcholine (POPC) parameters and charges used in this work were as described in our previous study (34). Starting from structures obtained in our previous work, we prepared systems with 256 POPC/112 cholesterol (30 mol % Chol), 256 POPC/112 25-HC (30 mol % 25-HC), 256 POPC/56 cholesterol (18 mol % Chol), 256 POPC/56 25-HC (18 mol % 25-HC), and 256 POPC molecules. The 0%, 18%, and 30% sterol concentration systems were chosen to cover the biologically relevant range of cholesterol concentrations, and to balance the requirements for sufficiently high oxysterol concentrations to detect membrane effects within our limited simulation time and sufficiently low oxysterol concentrations to have biological relevance. These bilayers were resolvated with 15850 SPC water molecules and 33 K^+ and Cl^- for an approximate molar concentration of 115 mM KCl. The simulations are summarized in Table 1. All MD simulations were performed using GROMACS version 3.3.1 or 4.0 (35,36), and the numbers of replicate simulations and durations are summarized in Table 1. Additional information, including simulation details, is provided in the Supporting Material.

Analysis methods

Standard structural analyses of the membrane (i.e., area, density profile, and hydrogen bonding), along with statistical significance testing, were performed as described in the Supporting Material.

We calculated the sterol orientations by defining molecular axes through the rigid sterol ring and evaluating angles of these molecular axes with respect to reference axes defined by the bilayer plane and normal axis, as described in our previous work (34). The main axis of the sterol ring can be seen in Fig. 1 for representative structures of cholesterol and 25-HC. We use two primary angles to describe sterol orientation: 1), the sterol tilt, which describes the angle of the steroid ring with respect to the membrane normal; and 2), the sterol twist, which describes the facing of the steroid ring with respect to the membrane surface. These angles vary from 0° to 180° for the tilt and −180° to 180° for the twist. The angles are projected onto a spherical surface, with the sterol tilt angle used as the spherical inclination and the sterol twist angle used as the spherical azimuth. This coordinate system puts parallel and antiparallel orientations at two opposite poles of the sphere, with perpendicular orientations with different facings along the equator.

We calculated the probability densities at each point of the spherical surface by first subdividing the surface into ~17,000 triangles. Sterol orientations from a given system composition were assigned to the closest triangle, and the total counts were divided by the triangular areas to obtain a final density. A threshold method was used to divide the distribution into viewable high- and low-probability density regions. The threshold was initially set to the highest local density value obtained for the system composition and progressively lowered until 10%, 25%, 50%, 75%, or 90% of all observed sterol orientations were found in regions of density higher than the threshold.

RESULTS

Membrane effects

Areas

The overall projected area of each system was calculated and used to determine the equilibration period of each system (details are presented in the Supporting Material). We obtained specific insight into the nature of the interactions between the two sterols by breaking down the total membrane areas into areas associated with each membrane component using solvent-accessible surface area (SASA) calculations. This allowed us to attribute changes in the total membrane area to changes in the areas of specific membrane

TABLE 1 Summary of all simulations performed and analyzed in this work

Composition	No. of initial simulations	No. of replica simulations	Cumulative simulation time (ns)
256 POPC	1	4	1200
256 POPC, 56 cholesterol	1	4	1200
256 POPC, 112 cholesterol	1	4	1200
256 POPC, 56 25-HC	1	4	1200
256 POPC, 112 25-HC	1	4	1200
256 POPC, 56 cholesterol, 56 25-HC	4	16	4800

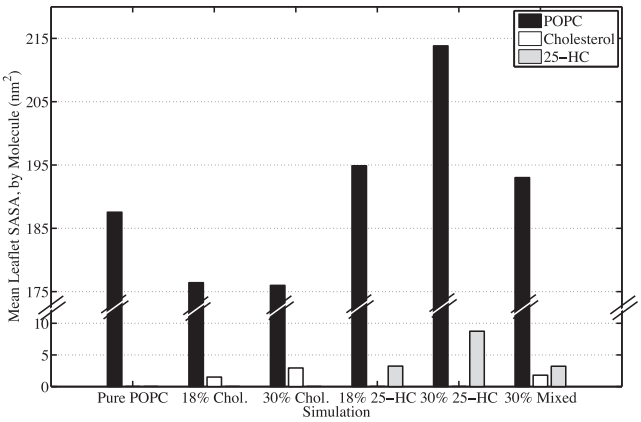

FIGURE 2 Bar plots showing the mean per-leaflet SASA of POPC (*black*), cholesterol (*white*), and 25-HC (*gray*) for each set of simulations. All comparisons between POPC surface areas are significant at 5% except those between the 18% and 30% cholesterol simulations (not significant) and those among the pure POPC, 18% 25-HC, and 30% mixed sterol simulations (not significant). Mean leaflet SASAs for POPC are 187.5 ± 4.7 nm^2 (pure POPC), 176.4 ± 4.0 nm^2 (18% cholesterol), 176.0 ± 3.5 nm^2 (30% cholesterol), 194.9 ± 3.9 nm^2 (18% 25-HC), 213.8 ± 3.6 nm^2 (30% 25-HC), and 193.0 ± 5.0 nm^2 (30% mixed sterols). Mean leaflet SASAs for cholesterol are 1.5 ± 0.3 nm^2 (18% cholesterol), 2.9 ± 0.3 nm^2 (30% cholesterol), and 1.8 ± 0.3 nm^2 (30% mixed sterols). Mean leaflet SASAs for 25-HC are 3.2 ± 0.4 nm^2 (18% 25-HC), 8.7 ± 0.7 nm^2 (30% 25-HC), and 3.2 ± 0.8 nm^2 (30% mixed sterols).

components. SASA calculations are not perfectly correlated with projected membrane areas because changes in membrane roughness and lipid projection from the surface can alter leaflet SASA without changing the projected areas.

The total contributions of POPC, cholesterol, and 25-HC to per-leaflet SASA were calculated as described in the Supporting Material and are shown in Fig. 2. Both the 18% and 30% concentrations of cholesterol reduce the POPC contribution to surface area by 11–12 nm^2. Because no further decrease in POPC SASA is observed at the higher concentration of cholesterol, a limit in phospholipid condensation by cholesterol must be reached between 0 and 30% cholesterol (37,38). The differences in cholesterol effects on the POPC SASA and membrane projected area suggest that cholesterol is either dampening the POPC projection from the bilayer or smoothing the POPC surface, thereby decreasing the POPC surface area faster than its projected area. The contribution of cholesterol itself to the leaflet surface area doubles from 1.5 nm^2 in the 18% cholesterol system to 2.9 nm^2 in the 30% system. Because the number of cholesterol molecules doubles as well, this indicates that cholesterol in POPC/cholesterol bilayers has a constant molecular SASA regardless of concentration.

The addition of 25-HC causes an increase in the POPC surface area. The 128 POPC molecules in each leaflet take up 7.3 nm^2 more surface area in the presence of 18% 25-HC, and 26.3 nm^2 more in the presence of 30% 25-HC. Moreover, 25-HC, in contrast to cholesterol, appears to not have a consistent mean molecular SASA over the range of concentrations examined. The contribution of 25-HC to the leaflet surface area more than doubles, indicating that at higher concentrations of 25-HC, the sterol becomes more exposed to solvent.

Areas of the 30% mixed sterol simulation are best examined by comparing the marginal effect of each sterol in the presence and absence of the other. In the absence of cholesterol, 18% 25-HC causes a 6.5 nm^2 increase in membrane projected area and a 7.4 nm^2 increase in phospholipid surface area (from 0% to 18% 25-HC). In the presence of cholesterol, the same number of oxysterol molecules cause a 9.1 nm^2 increase in projected area and a 16.6 nm^2 increase in phospholipid surface area (from 18% cholesterol to 30% mixed sterol). Similarly, without oxysterols present, 18% cholesterol causes a 0.1 nm^2 decrease in projected area and an 11.1 nm^2 decrease in phospholipid surface area (from 0% to 18% cholesterol), whereas in the presence of oxysterols, the same number of cholesterols cause an increase in projected area of 1.5 nm^2 and a decrease in phospholipid surface area of 1.9 nm^2 (from 18% 25-HC to 30% mixed sterol). This demonstrates that the membrane effects of oxysterols and cholesterol are nonadditive, suggesting that either oxysterols interfere with the ability of cholesterol to condense membranes or that cholesterol enhances the ability of oxysterols to expand membranes.

Densities

Mass density profiles for all simulations were calculated as described in the Supporting Material, and the densities for all simulations of the same composition were averaged. These mass density profiles are shown in Fig. 3. Each plot shows the solvent, phospholipid, and sterol density profiles for a single system composition. The general shape of each profile is similar among different system compositions: solvent density transitions smoothly from the bulk water density of ~975 kg m^{-3} to zero at the bilayer center, phospholipids show phosphate peaks at 1.7 to 2.2 nm and minimum densities at the bilayer center, and sterols have their major peaks further in at 1.5 to 1.7 nm.

Although the general shapes of the density profiles for all membrane compositions are similar, some differences are seen that provide insight into how sterols change membrane structure. Cholesterol thickens the membrane in a dose-dependent manner, shifting the major phosphate peak and the solvent density farther away from the bilayer center. It also narrows the phospholipid peaks, indicating more homogeneity in the position of the lipids and thus a more ordered membrane. At the same time, the minimum at the center of the bilayer deepens, indicating less intercalation between acyl chains of the two separate leaflets. 25-HC shifts solvent density and phospholipid peaks closer to the bilayer center, lowers phospholipid densities, and raises the minimum at the center of the bilayer. These changes show membrane thinning and lateral expansion, disordering of the phospholipid headgroups, and increases in acyl chain intercalation.

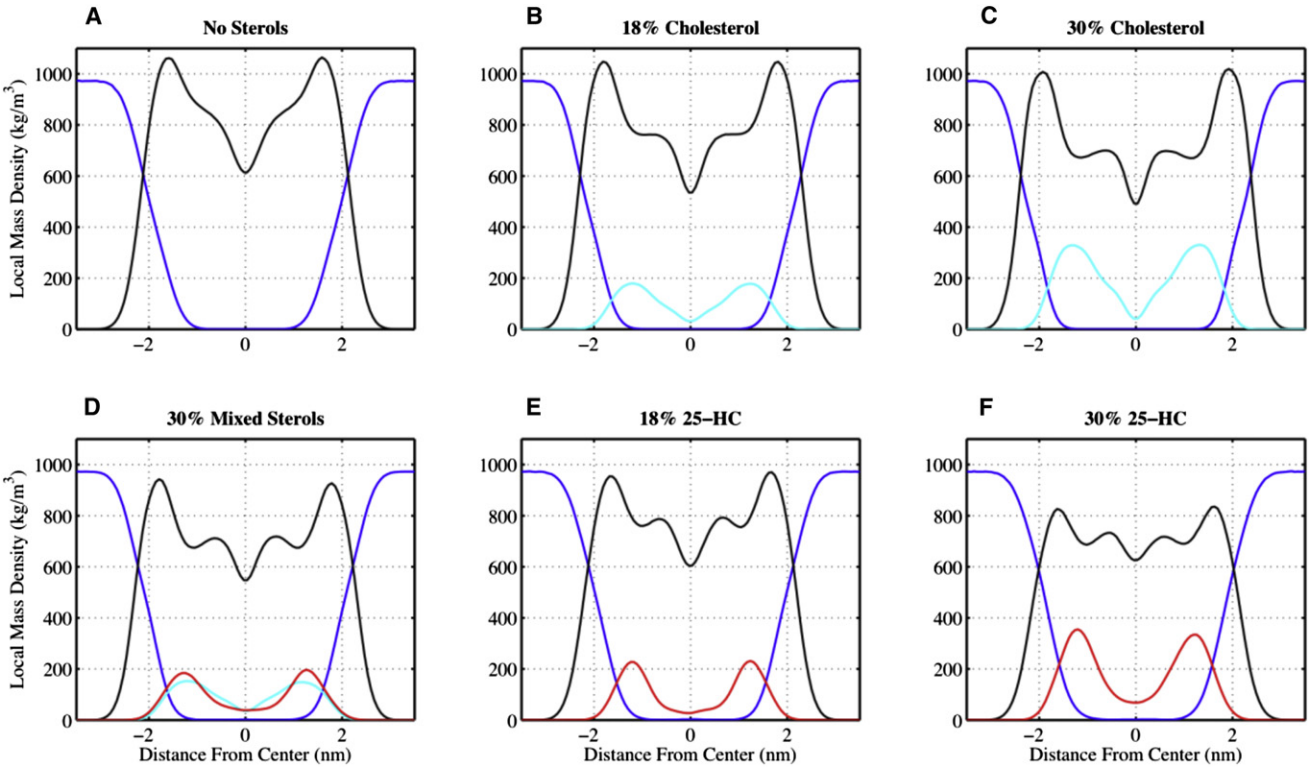

FIGURE 3 Mean component mass density profiles for simulations of pure POPC bilayers (*A*), 18% cholesterol bilayers (*B*), 30% cholesterol bilayers (*C*), 15% cholesterol, 15% 25-HC bilayers (*D*), 18% 25-HC bilayers (*E*), and 30% 25-HC bilayers (*F*). Solvent densities are shown in blue, POPC densities in black, cholesterol densities in cyan, and 25-HC densities in red.

The simulations containing both cholesterol and 25-HC show a mixture of these effects. The bilayer thickens slightly while the phosphate peak widens, and the opposing effects of 25-HC and cholesterol on acyl chain intercalation result in only small shifts in the bilayer minimum density with respect to the pure POPC bilayer.

Molecular effects

Molecular SASA

The SASA for each cholesterol molecule in each frame of the simulations was calculated as described in the Supporting Material. Cholesterol SASAs cluster around zero, making the probability of finding cholesterol molecules with very high surface areas quite low. To best compare SASA distributions for cholesterol in membranes of different composition, we calculated inverse cumulative probability distributions for cholesterol in the 18% cholesterol, 30% cholesterol, and 30% mixed sterol simulations (Fig. 4). Over the range of threshold SASAs, this distribution shows the fraction of all cholesterol molecules with SASAs larger than the threshold. There is no significant difference in the solvent exposure of cholesterol in the 18% and 30% cholesterol simulations. In the 30% mixed sterol simulation, cholesterol becomes significantly more exposed to solvent, with >20% of cholesterols having SASAs > 10 Å^2. Although the fraction of cholesterols with high SASAs is still not large, it becomes significantly larger in membranes containing 25-HC. We see a 33%, 80%, and 189% increase in the fraction of cholesterols with SASAs above thresholds of 10, 30, and 50 Å^2, respectively, in the presence of 25-HC.

We further examined cholesterol SASA in the absence of hydrophobic shielding by the phospholipid headgroup. After removing the POPC headgroups from the structures, we observed no significant differences in cholesterol SASA between the 18% and 30% cholesterol simulations and cholesterol in the 30% mixed sterol simulations, suggesting that the observed increase in cholesterol exposure in the presence of oxysterols was due to less-effective shielding by phospholipid headgroups.

Hydrogen bonding and solvation

The total number of cholesterol-solvent hydrogen bonds was calculated for each individual cholesterol. These results were pooled to find the fraction of cholesterols forming 0, 1, 2, 3, or 4 hydrogen bonds with solvent in each of the three cholesterol-containing system compositions. Probability histograms are shown in Fig. 5. As with cholesterol SASA, we find no significant differences in cholesterol-solvent hydrogen bonding between the 18% and 30%

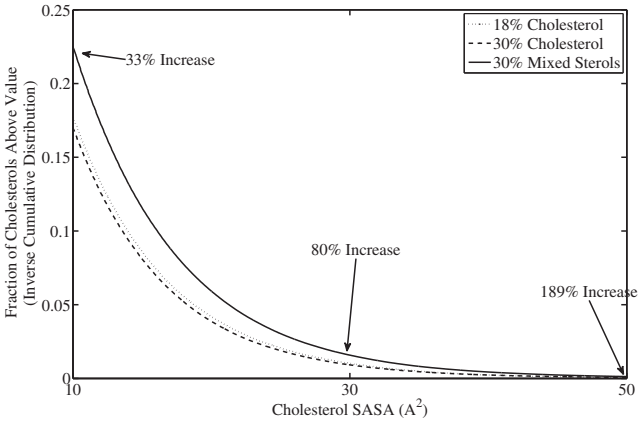

FIGURE 4 Inverse cumulative probability distributions for cholesterol SASA in the 18% cholesterol (*dotted*), 30% cholesterol (*dashed*) and 30% mixed sterol (*solid*) simulations. For each threshold SASA, the plot shows the fraction of cholesterol molecules present with areas larger than the threshold. The 30% mixed sterol distribution is significantly different at 1% from the cholesterol-only systems, and the low- and high-cholesterol systems are not significantly different from each other; 33% more cholesterol molecules have SASAs > 10 Å^2 in the mixed-sterol simulations than in the cholesterol-only simulations, 80% more have SASAs $>$ 30 Å^2, and 189% more have SASAs > 50 Å^2.

cholesterol. Cholesterol in these cholesterol/POPC simulations prefers to hydrogen-bond with a single water molecule, with <5% forming no solvent hydrogen bonds and only ~15% forming more than one. In the 30% mixed sterol simulations, cholesterol forms significantly more hydrogen bonds with water. In the presence of 25-HC, most cholesterol molecules prefer to hydrogen-bond with multiple water molecules. This demonstrates that the increase in cholesterol SASA observed in the presence of 25-HC is accompanied by increased interactions with solvent molecules.

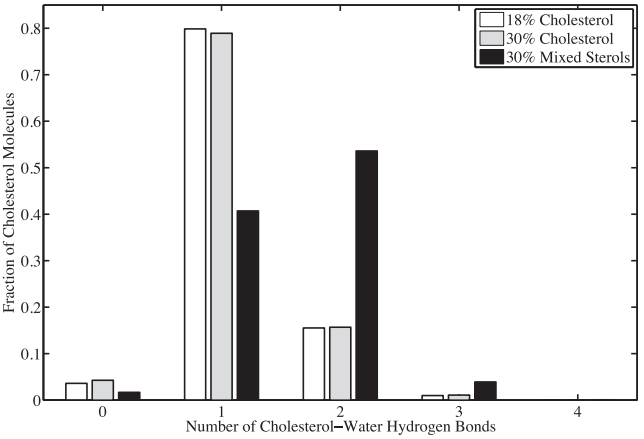

FIGURE 5 Histograms showing the number of cholesterol-water hydrogen bonds for cholesterol molecules in the 18% cholesterol (*white*), 30% cholesterol (*gray*), and 30% mixed-sterol (*black*) simulations. The 30% mixed sterol distribution is significantly different at 1% from the cholesterol-only systems, and the low- and high-cholesterol systems are not significantly different from each other.

Sterol positions

Although an examination of individual cholesterol SASA and hydrogen bonding shows that cholesterol becomes more exposed to solvent in the presence of 25-HC, it does not reveal how this increased exposure occurs. Increased exposure may be due to movement of cholesterol out of the bilayer into the solvent, or to an opening of the bilayer structure that allows solvent to penetrate. To examine this, we calculated the positions of cholesterol molecules with respect to the interface between the solvent and the bilayer. Interface positions were calculated as described in the Supporting Material. The probability distributions for cholesterol hydroxyl positions with respect to the interface are shown in Fig. 6. We find that the distributions of cholesterol positions in the 18% and 30% simulations are not significantly different. Cholesterol prefers to position its hydroxyl group in the bilayer between 2.5 and 5 Å below the water interface, with a median depth of 3.6 Å for both 18% and 30% cholesterol systems. In the 30% mixed sterol simulations, cholesterol shifts significantly closer to the water interface, with a median depth of 2.8 Å. Although the shift is small compared with the width of the distributions, it results in a large change in the fraction of cholesterol molecules positioned above the water interface. Only 3–4% of cholesterols in the 18% and 30% cholesterol simulations are located above the water interface, compared with >8% in the 30% mixed sterol simulations. The cholesterol position results show that the increased exposure of cholesterol to solvent induced by 25-HC, as shown in the cholesterol SASA and hydrogen-bonding data, is due to movement of cholesterol out of the bilayer rather than to a change in bilayer structure that allows increased solvent penetration.

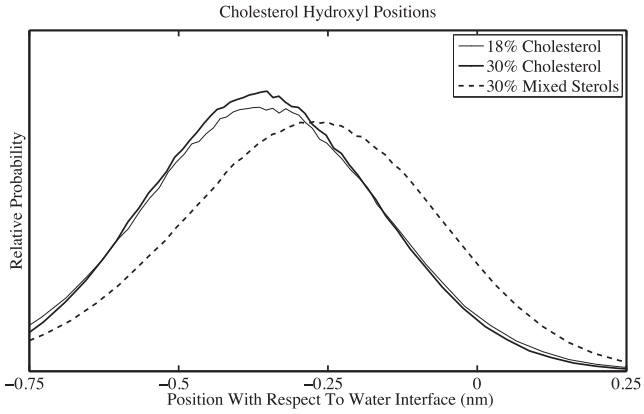

FIGURE 6 Probability distributions for finding the oxygen of the cholesterol hydroxyl at a given position with respect to the water-bilayer interface. Shown for cholesterol in the 18% cholesterol (*thin solid*), 30% cholesterol (*thick solid*), and 30% mixed sterol (*dashed*) simulations. The 30% mixed sterol distribution is significantly different at 1% from the cholesterol-only systems, and the low- and high-cholesterol systems are not significantly different from each other.

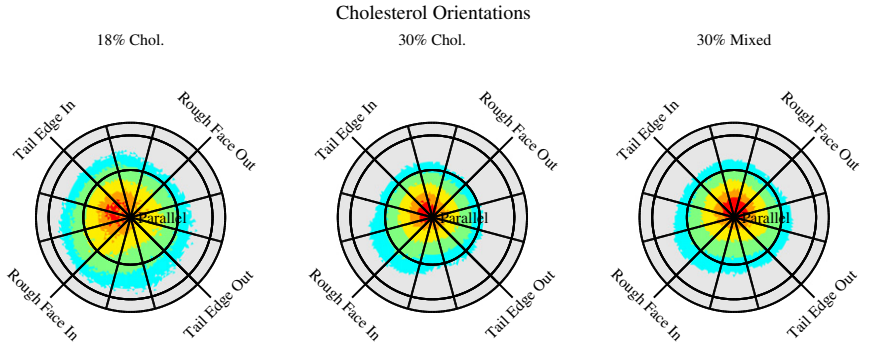

FIGURE 7 Spherical probability density plots of cholesterol orientations in the 18% cholesterol, 30% cholesterol, and 30% mixed-sterol simulations. The regions of highest density are labeled in red (containing 10% of all sterols), with progressively lower densities labeled in orange (15% of sterols), yellow (25% of sterols), green (25% of sterols), and cyan (15% of sterols). The center pole denotes parallel orientations, with radiating circles denoting 30°, 60°, and 90° sterol tilt angles. Radiating lines denote sterol twist angles, with adjacent lines separated by 30°. The rough face and tail edge of the sterols are shown in Fig. 1.

Sterol orientations

In a previous work we examined the differential effects of 25-HC and cholesterol on membrane behavior and found significant differences in the orientations of the two sterols within bilayers (34). We suggested that these differential orientations might be responsible for their effects on membrane structure, and in particular that the interfacial orientations adopted by 25-HC could be responsible for the marked increase in membrane area observed in 25-HC-containing membranes. To further examine this hypothesis, in this work we calculated the distributions of the orientations of both cholesterol and 25-HC in the 18% single sterol, 30% single sterol, and 30% mixed sterol simulations. We also calculated the sterol tilt and twist for each sterol molecule in these simulations to describe each sterol's orientation. Contour plots of spherical distributions of these orientations are shown in Fig. 7 for cholesterol and Fig. 8 for 25-HC.

An examination of the cholesterol results shows few differences in cholesterol orientations among the three sets of simulations. In all cases, cholesterol prefers parallel orientations, with >60% of cholesterol molecules having ring tilts of <30°. There is a slight shift toward a tighter distribution around the preferred parallel orientation at higher sterol concentrations. Because this shift is seen in both the 30% cholesterol simulations and the 30% mixed sterol simulations, it appears to be dependent on the general sterol concentration.

An examination of the 25-HC orientations shows two preferred orientations: parallel and interfacial. We define a parallel orientation as one with a ring tilt of <30°, and an interfacial orientation as one with a ring tilt between 40° and 80° and a ring twist between −45° and 60°. At the low 18% concentration, 25-HC prefers to adopt primarily interfacial orientations. This orientation allows both hydroxyl groups to interact with solvent by tilting the hydroxylated tail toward the water interface. Although this interfacial orientation is dominant, the distribution is broad, with a wide variety of other available orientations, including inverted orientations with the sterol tail at the water interface and the steroid ring buried in the bilayer (data not shown). Approximately 35% of oxysterols are found in interfacial orientations; only 13% are found in parallel orientations and the remainder are observed in various alternative conformations. At the higher 30% 25-HC concentration, there is a shift from alternative to parallel conformations, with 19% of 25-HC molecules adopting parallel orientations similar to that of cholesterol, whereas the fraction in interfacial orientations does not significantly change. This may be due to saturation of possible occupancy sites that prevents further alternative orientations and leads excess 25-HC to adopt parallel orientations. In the 30% mixed sterol simulation, we see an even larger shift toward parallel orientations, with 31% of 25-HC molecules adopting parallel orientations. In this case, the increase in parallel

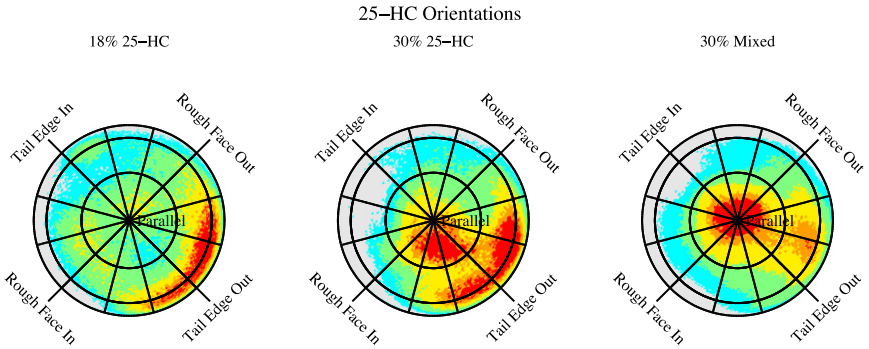

FIGURE 8 Spherical distribution plots of 25-HC orientations in the 18% 25-HC, 30% 25-HC, and 30% mixed-sterol simulations. The regions of highest density are labeled in red (containing 10% of all sterols), with progressively lower densities labeled in orange (15% of sterols), yellow (25% of sterols), green (25% of sterols), and cyan (15% of sterols). The center pole denotes parallel orientations, with radiating circles denoting 30°, 60°, and 90° sterol tilt angles. Radiating lines denote sterol twist angles, with adjacent lines separated by 30°. The rough face and tail edge of the sterols are shown in Fig. 1.

orientations is compensated for by a decrease in interfacial orientations, with only 24% of oxysterols adopting interfacial orientations.

On the basis of our earlier work, we expected the presence of 25-HC interfacial orientations to correlate with membrane expansion. This appears to be the case in the absence of cholesterol: in the 18% and 30% 25-HC simulations, the fraction of oxysterols in interfacial orientations is approximately the same. This increase in total interfacial oxysterols correlates with the increase in membrane expansion between the low and high 25-HC concentration simulations. In the presence of cholesterol, however, this correlation is no longer seen. Although significantly fewer oxysterols in the mixed sterol simulations are found in interfacial orientations than in the 18% 25-HC simulations, these oxysterols cause a larger increase in membrane area.

DISCUSSION

In this study we provide evidence for indirect interactions between cholesterol and 25-HC in POPC membranes. In mixed bilayers, the two sterols distribute evenly throughout the bilayer, without phase separation, as shown by radial distribution functions of cholesterol-25-HC distances (Supporting Material). When added to POPC bilayers at low concentrations, 25-HC expands the bilayers, increasing the solvent exposure of nearby phospholipids. The same concentration added to bilayers containing cholesterol causes an even larger increase in POPC expansion. Cholesterol is well known to promote condensation of nearby phospholipids, decreasing their per-lipid area (10,11). Phospholipid surface area calculations demonstrated that the addition of cholesterol causes a much smaller decrease in phospholipid surface area in membranes containing 25-HC than in membranes without 25-HC, suggesting that the presence of 25-HC interferes with the ability of cholesterol to condense bilayers. In addition to influencing how cholesterol alters membrane structure, 25-HC also changes cholesterol conformations and positions. In the presence of 25-HC, cholesterol shifts toward more-exposed conformations, positioning itself closer to the bilayer surface and becoming more exposed to solvent.

On the basis of our earlier findings, we predicted that 25-HC would induce more membrane expansion in the presence of cholesterol, and hypothesized that this would be caused by conformational and orientational shifts in 25-HC (34). We proposed that 25-HC causes membrane expansion through its adoption of interfacial conformations, that the presence of cholesterol would cause 25-HC to favor these interfacial conformations, and hence that 25-HC would has a larger expansive effect on membranes containing cholesterol. First, assuming that membranes can contain only a limited number of upright sterols, we reasoned that cholesterol would compete with 25-HC for access to these upright orientations, driving 25-HC toward interfacial orientations. However, we find that this predicted conformational shift does not occur. Instead, 25-HC shifts away from interfacial orientations in cholesterol-containing membranes. Rather than competing with 25-HC for upright orientations, cholesterol alters membrane structure in such a way as to energetically favor upright conformations. The loss of correlation between interfacial oxysterol concentration and membrane expansion in the presence of cholesterol suggests that either interfacial oxysterols result from rather than directly cause area expansion, or cholesterol increases the ability of interfacial oxysterols to induce area expansion.

A potential consequence of these shifts in 25-HC orientation could be a change in oxysterol-induced membrane permeability. We previously speculated that the hydrogen-bonded oxysterol clusters formed by upright 25-HC molecules are the cause of oxysterol-induced increases in membrane permeability (34). Clusters of oxysterol hydroxyl groups in the center of the bilayer would lower the desolvation penalty of passing small polar molecules through the bilayer by offering alternative hydrogen-bonding sites. The shift in oxysterol orientations from interfacial to upright conformations we observed in the presence of cholesterol would also cause an increase in the number of available hydrogen-bonding sites in the interior of the bilayer, further lowering the barrier to small-molecule permeation of the bilayer. Thus, we hypothesize that the observed increase in membrane permeability induced by 25-HC will be larger in membranes containing cholesterol than in those without.

It has been hypothesized that membrane cholesterol exists in both complexed and free or activated forms (34). Although complexed cholesterol is tightly bound to phospholipids and is unavailable to enzymes or binding partners, activated cholesterol is available to partners such as cholesterol oxidase and extramembrane acceptors such as cyclodextrin and lipoproteins (28). Under normal conditions, the availability of cholesterol is determined by the capacity of membrane phospholipids to form complexes with cholesterol. Addition of cholesterol past membrane capacity increases the pool of uncomplexed free cholesterol with higher activity (28). A wide range of amphipaths, including alcohols, fatty acids, and ketones, have been shown to increase the fraction of activated cholesterol when added to membranes (39).

We found changes in cholesterol position and solvent exposure in 25-HC-containing bilayers consistent with cholesterol activation. In the absence of 25-HC, the cholesterol hydroxyl group has a mean position slightly below the bilayer/water interface. The addition of 25-HC to the membrane shifts the cholesterol hydroxyl toward the interface by nearly an Ångström. The change in cholesterol position is accompanied by increased exposure of cholesterol to solvent, as measured by cholesterol SASA and cholesterol-solvent hydrogen bonding. These findings demonstrate that there is a reduction in the shielding of the largely hydrophobic cholesterol by surrounding phospholipid headgroups.

Although we find changes consistent with cholesterol activation, we do not find any direct disruption of cholesterol-phospholipid interactions. In the absence of 25-HC, almost all (>95%) cholesterol molecules form a single hydrogen bond with a phospholipid, and this does not change when 25-HC is added (data not shown). Further, radial distribution functions for cholesterol-POPC distances are very similar between cholesterol-only and mixed sterol bilayers, indicating that cholesterol is not displaced laterally from neighboring phospholipids by 25-HC (Fig. S2 and Fig. S3). We also found that measuring cholesterol solvent exposure in the absence of phospholipid headgroups showed no significant changes upon addition of 25-HC. Together, these results suggest that the increased availability and exposure of cholesterol induced by 25-HC is caused not by disruption of cholesterol-phospholipid complexes, but by oxysterol interference with phospholipid shielding of cholesterol.

It is plausible that the oxysterol-induced expansion of membrane bilayers is a biologically relevant signaling mechanism. Although oxysterols are only present at quite low concentrations across the entire cell, the spatial distribution of oxysterols within the cell is not known, and in the region around oxysterol-producing enzymes or sterol-binding proteins, local oxysterol concentrations may approach the concentrations represented in our simulations. Locally elevated concentrations of oxysterols could cause changes in membrane structure sufficient to alter membrane protein structure and activity. The ability of cholesterol to enhance the expansive effect of side-chain oxysterols on membranes may be relevant, with cholesterol serving not only as a substrate for oxysterol production but also as an enhancer of oxysterol-induced membrane effects or oxysterol-protein interactions.

Oxysterol-induced cholesterol activation provides another mechanism through which 25-HC can act in a non-enantioselective manner. Increased active cholesterol levels in the plasma membrane could be responsible for the increased trafficking of cholesterol when exogenous 25-HC is added to cells (28). Side-chain oxysterols present in the ER could activate cholesterol, increasing its availability to sterol-sensing machinery in the ER and modulating the regulatory response to ER cholesterol levels. On the basis of this signaling model, we predict that 25-HC-mediated suppression of SREBP maturation will depend on the presence of cholesterol and be greatly diminished in cholesterol-starved cells. We also anticipate that 25-HC will increase the availability of cholesterol to cholesterol oxidase and cyclodextrin in a dose-dependent manner.

Further study of these systems is necessary to fully understand the interacting effects of cholesterol and oxysterols on membrane behavior and lipid structure. The dose dependence of oxysterol activation of cholesterol is not yet clear. An unresolved question is, as oxysterol concentration is lowered, are all cholesterol molecules affected equally, or are some cholesterol populations affected differentially? It seems likely that oxysterol effects are local to nearby cholesterol molecules within a few solvation shells, but at the concentrations used here, this question cannot be resolved. Further, at the cholesterol concentrations used, we found no obvious division of cholesterol molecules into activated and complexed pools. This is not surprising, however, given that in experimental studies of POPC membranes, cholesterol concentration must rise above 30% to begin transitioning into the activated pool (27,28). Further simulations would be useful for resolving these questions. For example, simulations of mixed sterol bilayers at low oxysterol concentrations would demonstrate whether oxysterol effects are local, and simulations at higher cholesterol concentrations would show us whether complexed and activated pools can be observed in our simulations.

SUPPORTING MATERIAL

Additional methods, results, figures, and references are available at http://www.biophysj.org/biophysj/supplemental/S0006-3495(11)00005-1.

We thank Doug Covey, Katie Henzler-Wildman, and George Bonheyo for helpful discussions and feedback.

This work was supported by the National Institutes of Health (grants U54 CA11934205 and R01 GM069702 to N.A.B., and R01 HL067773 to D.S.O.). B.N.O. was supported by a Cellular and Molecular Biology Training Grant (NIH T32 GM007067). Computational resources were provided by the Texas Advanced Computing Center through Teragrid grants TG-MCB060053 and TG-MCA08X003, as well as the National Biomedical Computation Resource (NIH P41 RR0860516).

REFERENCES

1. Ohvo-Rekilä, H., B. Ramstedt, …, J. P. Slotte. 2002. Cholesterol interactions with phospholipids in membranes. *Prog. Lipid Res.* 41:66–97.
2. van Meer, G., D. R. Voelker, and G. W. Feigenson. 2008. Membrane lipids: where they are and how they behave. *Nat. Rev. Mol. Cell Biol.* 9:112–124.
3. Liscum, L., and N. J. Munn. 1999. Intracellular cholesterol transport. *Biochim. Biophys. Acta.* 1438:19–37.
4. Kuwabara, P. E., and M. Labouesse. 2002. The sterol-sensing domain: multiple families, a unique role? *Trends Genet.* 18:193–201.
5. Chang, T. Y., C. C. Y. Chang, …, Y. Yamauchi. 2006. Cholesterol sensing, trafficking, and esterification. *Annu. Rev. Cell Dev. Biol.* 22:129–157.
6. Epand, R. M. 2006. Cholesterol and the interaction of proteins with membrane domains. *Prog. Lipid Res.* 45:279–294.
7. Chiang, J. Y. L. 2004. Regulation of bile acid synthesis: pathways, nuclear receptors, and mechanisms. *J. Hepatol.* 40:539–551.
8. Nezil, F. A., and M. Bloom. 1992. Combined influence of cholesterol and synthetic amphiphillic peptides upon bilayer thickness in model membranes. *Biophys. J.* 61:1176–1183.
9. Purdy, P. H., M. H. Fox, and J. K. Graham. 2005. The fluidity of Chinese hamster ovary cell and bull sperm membranes after cholesterol addition. *Cryobiology.* 51:102–112.
10. Hung, W. C., M. T. Lee, …, H. W. Huang. 2007. The condensing effect of cholesterol in lipid bilayers. *Biophys. J.* 92:3960–3967.
11. Warschawski, D. E., and P. F. Devaux. 2005. Order parameters of unsaturated phospholipids in membranes and the effect of

cholesterol: a 1H-13C solid-state NMR study at natural abundance. *Eur. Biophys. J.* 34:987–996.

12. Martinez, G. V., E. M. Dykstra, …, M. F. Brown. 2002. NMR elastometry of fluid membranes in the mesoscopic regime. *Phys. Rev. E.* 66:050902.
13. Endress, E., H. Heller, …, T. M. Bayerl. 2002. Anisotropic motion and molecular dynamics of cholesterol, lanosterol, and ergosterol in lecithin bilayers studied by quasi-elastic neutron scattering. *Biochemistry.* 41:13078–13086.
14. Incardona, J. P., and S. Eaton. 2000. Cholesterol in signal transduction. *Curr. Opin. Cell Biol.* 12:193–203.
15. Edidin, M. 2003. The state of lipid rafts: from model membranes to cells. *Annu. Rev. Biophys. Biomol. Struct.* 32:257–283.
16. Lundbaek, J. A., O. S. Andersen, …, C. Nielsen. 2003. Cholesterol-induced protein sorting: an analysis of energetic feasibility. *Biophys. J.* 84:2080–2089.
17. McIntosh, T. J., and S. A. Simon. 2006. Roles of bilayer material properties in function and distribution of membrane proteins. *Annu. Rev. Biophys. Biomol. Struct.* 35:177–198.
18. Shimano, H., J. D. Horton, …, J. L. Goldstein. 1996. Overproduction of cholesterol and fatty acids causes massive liver enlargement in transgenic mice expressing truncated SREBP-1a. *J. Clin. Invest.* 98:1575–1584.
19. Goldstein, J. L., and M. S. Brown. 1990. Regulation of the mevalonate pathway. *Nature.* 343:425–430.
20. Janowski, B. A., M. J. Grogan, …, D. J. Mangelsdorf. 1999. Structural requirements of ligands for the oxysterol liver X receptors LXRα and LXRβ. *Proc. Natl. Acad. Sci. USA.* 96:266–271.
21. Janowski, B. A., P. J. Willy, …, D. J. Mangelsdorf. 1996. An oxysterol signalling pathway mediated by the nuclear receptor LXRα. *Nature.* 383:728–731.
22. Brown, M. S., and J. L. Goldstein. 1997. The SREBP pathway: regulation of cholesterol metabolism by proteolysis of a membrane-bound transcription factor. *Cell.* 89:331–340.
23. Horton, J. D., J. L. Goldstein, and M. S. Brown. 2002. SREBPs: activators of the complete program of cholesterol and fatty acid synthesis in the liver. *J. Clin. Invest.* 109:1125–1131.
24. Gil, G., J. R. Faust, …, M. S. Brown. 1985. Membrane-bound domain of HMG CoA reductase is required for sterol-enhanced degradation of the enzyme. *Cell.* 41:249–258.
25. Cheng, D., C. C. Y. Chang, …, T. Y. Chang. 1995. Activation of acyl-coenzyme A:cholesterol acyltransferase by cholesterol or by oxysterol in a cell-free system. *J. Biol. Chem.* 270:685–695.
26. Norlin, M., and K. Wikvall. 2007. Enzymes in the conversion of cholesterol into bile acids. *Curr. Mol. Med.* 7:199–218.
27. Lange, Y., J. Ye, and T. L. Steck. 2004. How cholesterol homeostasis is regulated by plasma membrane cholesterol in excess of phospholipids. *Proc. Natl. Acad. Sci. USA.* 101:11664–11667.
28. Lange, Y., and T. L. Steck. 2008. Cholesterol homeostasis and the escape tendency (activity) of plasma membrane cholesterol. *Prog. Lipid Res.* 47:319–332.
29. Lange, Y., J. Ye, …, T. L. Steck. 1999. Regulation of endoplasmic reticulum cholesterol by plasma membrane cholesterol. *J. Lipid Res.* 40:2264–2270.
30. Yabe, D., M. S. Brown, and J. L. Goldstein. 2002. Insig-2, a second endoplasmic reticulum protein that binds SCAP and blocks export of sterol regulatory element-binding proteins. *Proc. Natl. Acad. Sci. USA.* 99:12753–12758.
31. Yang, Q., R. Alemany, J. Casas, K. Kitajka, S. M. Lanier, and P. V. Escribá. 2005. Influence of the membrane lipid structure on signal processing via G protein-coupled receptors. *Mol. Pharmacol.* 68:210–217.
32. Yang, T., P. J. Espenshade, …, M. S. Brown. 2002. Crucial step in cholesterol homeostasis: sterols promote binding of SCAP to INSIG-1, a membrane protein that facilitates retention of SREBPs in ER. *Cell.* 110:489–500.
33. Gale, S. E., E. J. Westover, …, D. S. Ory. 2009. Side chain oxygenated cholesterol regulates cellular cholesterol homeostasis through direct sterol-membrane interactions. *J. Biol. Chem.* 284:1755–1764.
34. Olsen, B. N., P. H. Schlesinger, and N. A. Baker. 2009. Perturbations of membrane structure by cholesterol and cholesterol derivatives are determined by sterol orientation. *J. Am. Chem. Soc.* 131:4854–4865.
35. Berendsen, H. J. C., D. van der Spoel, and R. van Drunen. 1995. GROMACS: a message-passing parallel molecular dynamics implementation. *Comput. Phys. Commun.* 91:43–56.
36. Lindahl, E., B. Hess, and D. van der Spoel. 2001. GROMACS 3.0: a package for molecular simulation and trajectory analysis. *J. Mol. Model.* 7:306–317.
37. Chiu, S. W., E. Jakobsson, …, H. L. Scott. 2002. Cholesterol-induced modifications in lipid bilayers: a simulation study. *Biophys. J.* 83:1842–1853.
38. Pandit, S. A., S. W. Chiu, …, H. L. Scott. 2008. Cholesterol packing around lipids with saturated and unsaturated chains: a simulation study. *Langmuir.* 24:6858–6865.
39. Lange, Y., J. Ye, …, T. L. Steck. 2009. Activation of membrane cholesterol by 63 amphipaths. *Biochemistry.* 48:8505–8515.